Science Advances
AAAS

Supplementary Materials for

Rejuvenation of peripheral immune cells attenuates Alzheimer's disease-like pathologies and behavioral deficits in a mouse model

Pu-Yang Sun *et al.*

Corresponding author: Yan-Jiang Wang, yanjiang_wang@tmmu.edu.cn; Jun Wang, qywangjun@163.com

Sci. Adv. **10**, eadl1123 (2024)
DOI: 10.1126/sciadv.adl1123

The PDF file includes:

Other Supplementary Material for this manuscript includes the following:

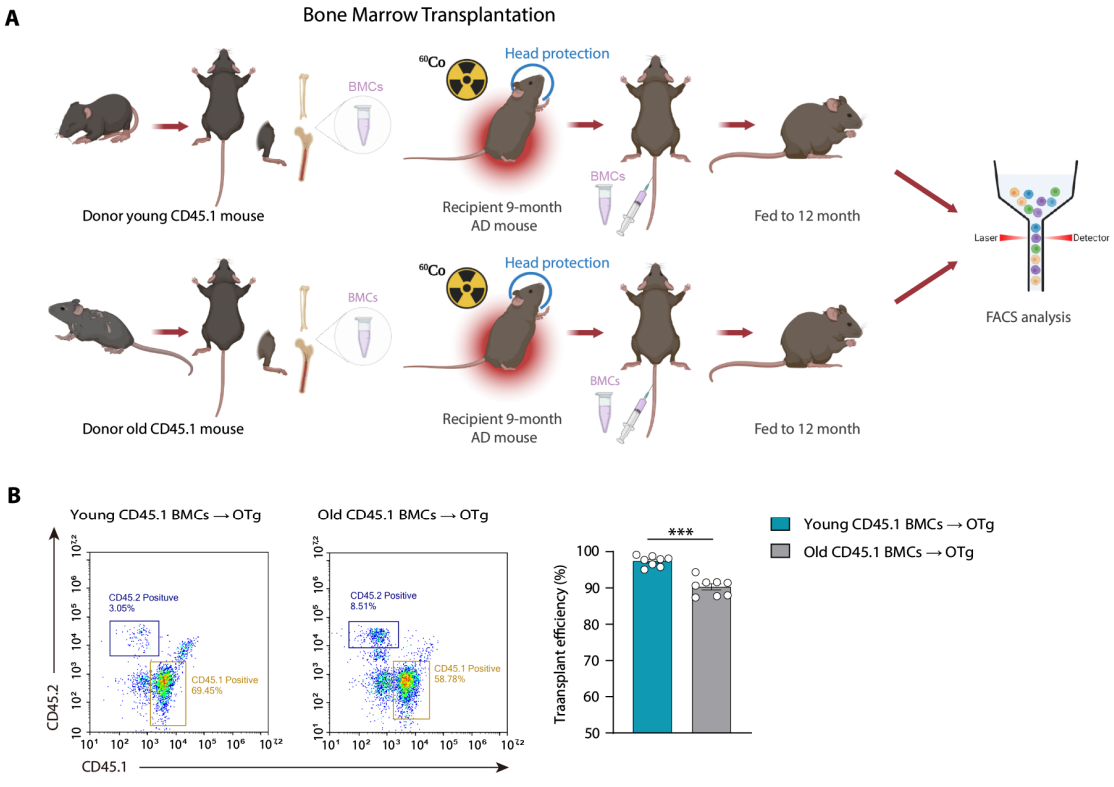

Fig. S1. Analysis of the bone marrow transplantation efficiency by flow cytometry.

(**A**) Schematic presentation of the experimental design used to investigate transplantation efficiency. $CD45.1^+$ WT mice were used as donors instead of $CD45.2^+$ *APP/PS1* mice to distinguish between donor and recipient origins of PBMCs. (**B**) Flow cytometry (left) and quantification (right) showing the transplant efficiency. Transplant efficiency was calculated as $CD45.1^+/(CD45.1^+ + CD45.2^+)$. Un-paired t-test. ***indicates $p < 0.001$, and the error bars are the SEMs.

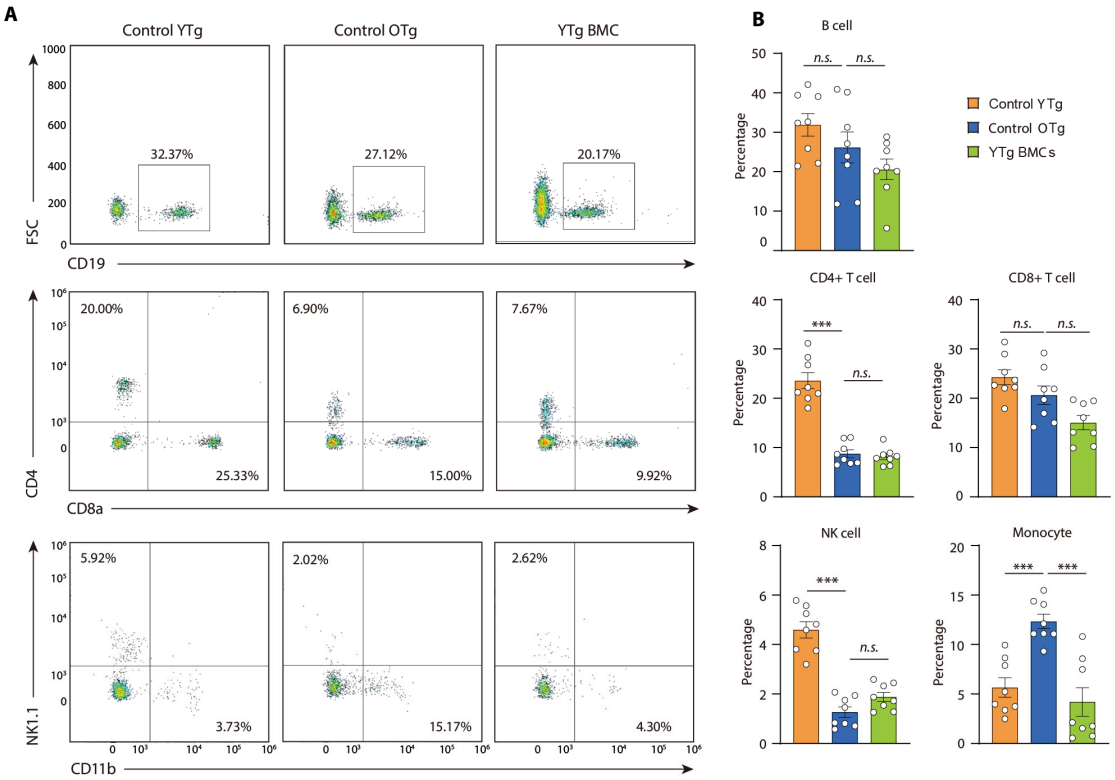

Fig. S2. Quantification of the cell proportion of the main immune cell types in PBMCs by flow cytometry. (**A**) Representative FACS plot of marker gene staining of different immune cell types. (**B**) Quantification showing the percentages of B cells, CD4+ cells, CD8+ cells, NK cells and monocytes in peripheral blood from control YTg, control OTg and YTg BMC mice. One-way ANOVA. ***indicates $p < 0.001$, and the error bars are the SEMs.

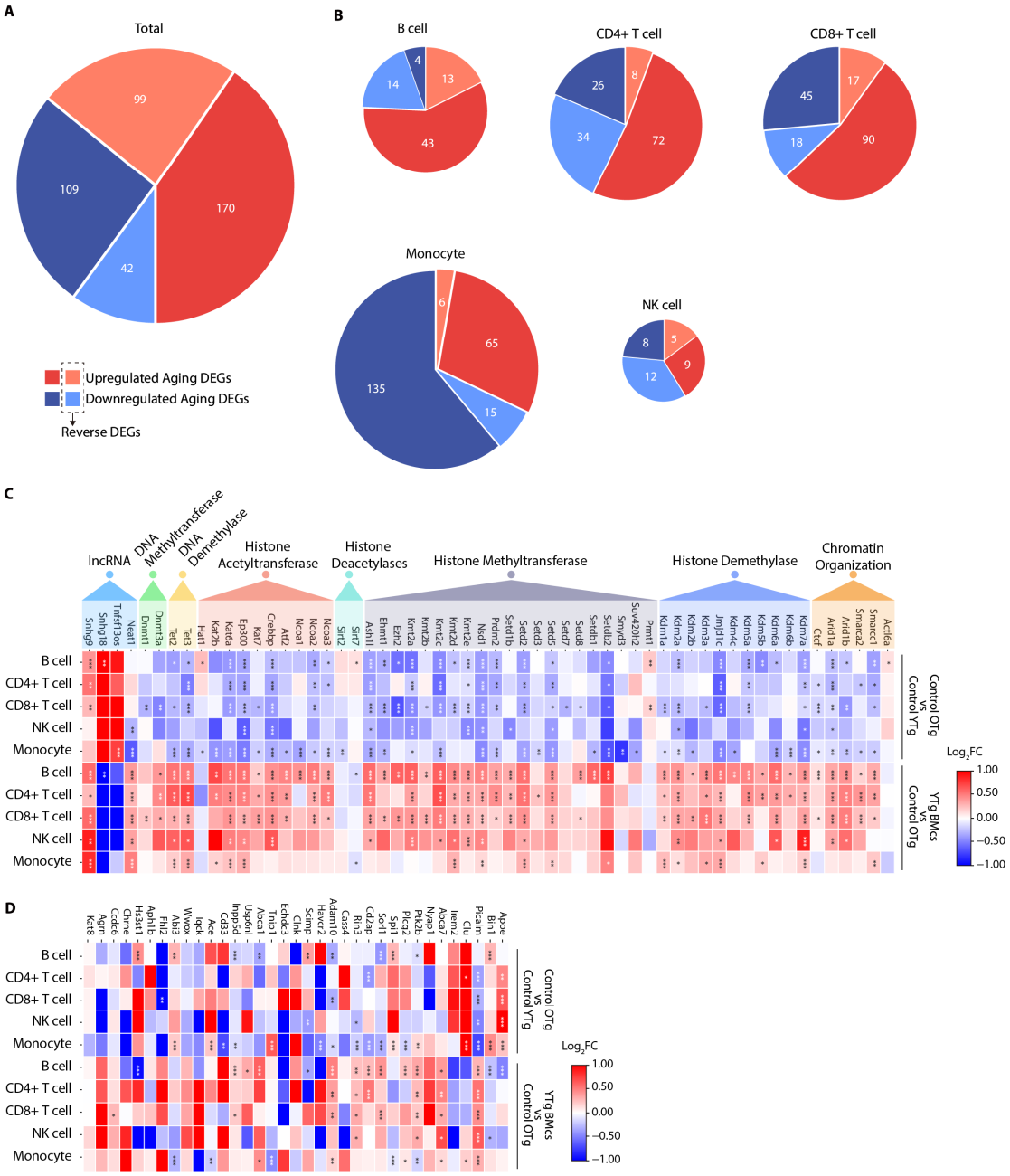

Fig. S3. Young BMT reverse gene expression in senescent immune cells. (**A**) Summary of the total aging and reverse DEGs in PBMCs. The red and pink parts represent the total upregulated aging DEGs, while the pink part represents those whose expression was reversed after young BMT. (**B**) Summary of the aging and reverse DEGs in each subcell-type. (**C**) Heatmap of the epigenetics regulation associated genes in

each cell type. The color key indicates the Log_2FC value. (**D**) Heatmap of the top 45 AD risk genes in aging and BMT of B cells, CD4+ T cells, CD8+ T cells, NK cells and monocytes. The color indicates the Log_2FC values. *indicates $p < 0.05$, **indicates $p < 0.01$, ***indicates $p < 0.001$.

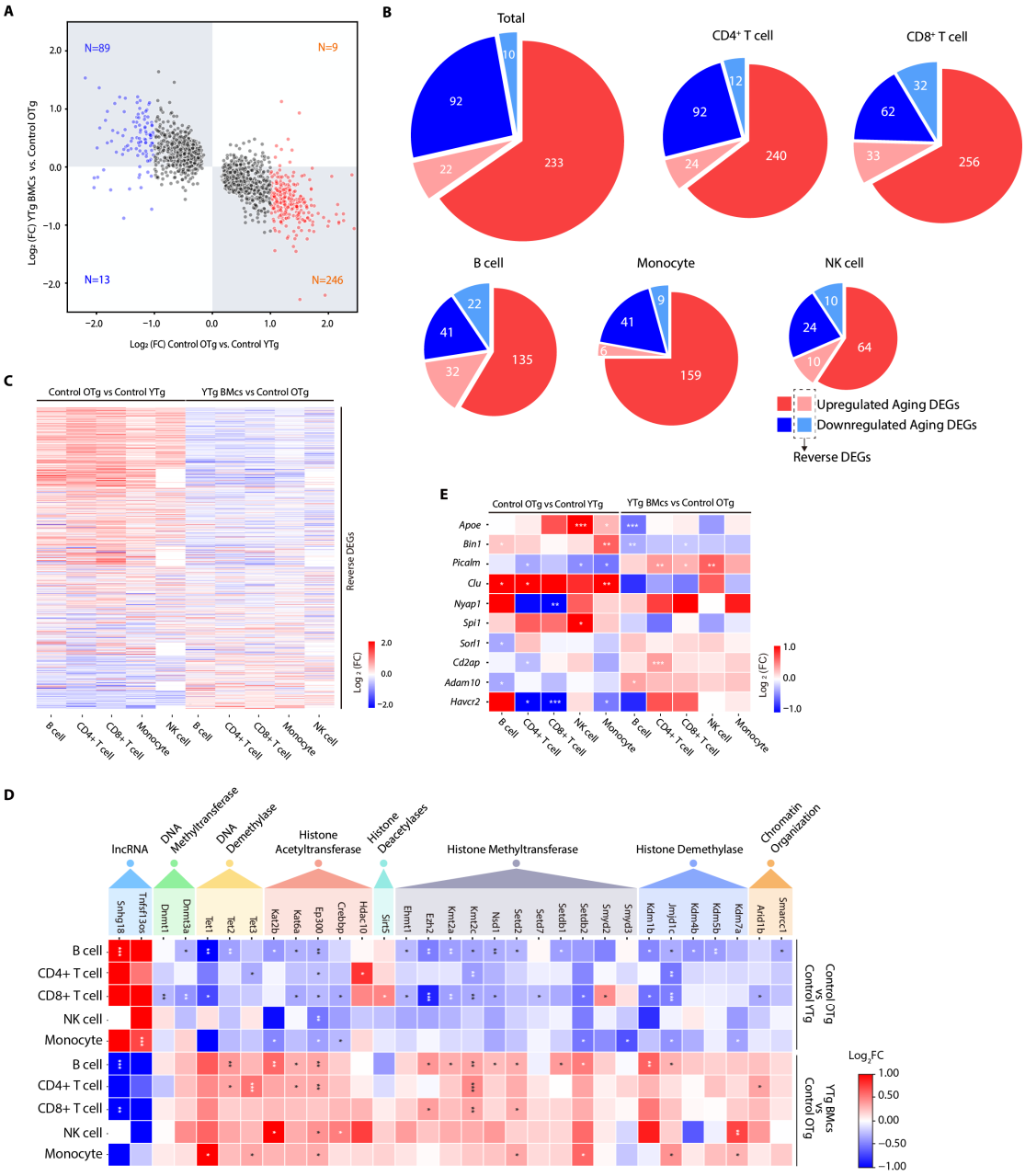

Fig. S4. Aging and reverse-DEGs in multiple cell types of PBMCs analyzed by pseudobulk DEG analysis. (A) Scatter plot of the general aging DEGs (cut-off by $p<0.05$, $Log_2FC>1.0$) in PBMCs. (B) Summary of the total and each sub cell-type aging and reverse DEGs in PBMCs. The red and pink parts represent the total upregulated aging DEGs, while the pink part represents those whose expression was reversed after young BMT. (C) Heatmap of the reversed DEGs in each cell type alongside the young

BMT. The color key indicates the Log_2FC values. (D) Heatmap of the epigenetics-related genes in aging and BMT of B cells, CD4+ T cells, CD8+ T cells, NK cells and monocytes. (E) The expression of differentially expressed AD risk genes in aging and BMT of B cells, CD4+ T cells, CD8+ T cells, NK cells and monocytes. The color indicates the log2FC values. *indicates $p < 0.05$; **indicates $p < 0.01$, ***indicates $p < 0.001$. The error bars are the SEMs. FC: fold change.

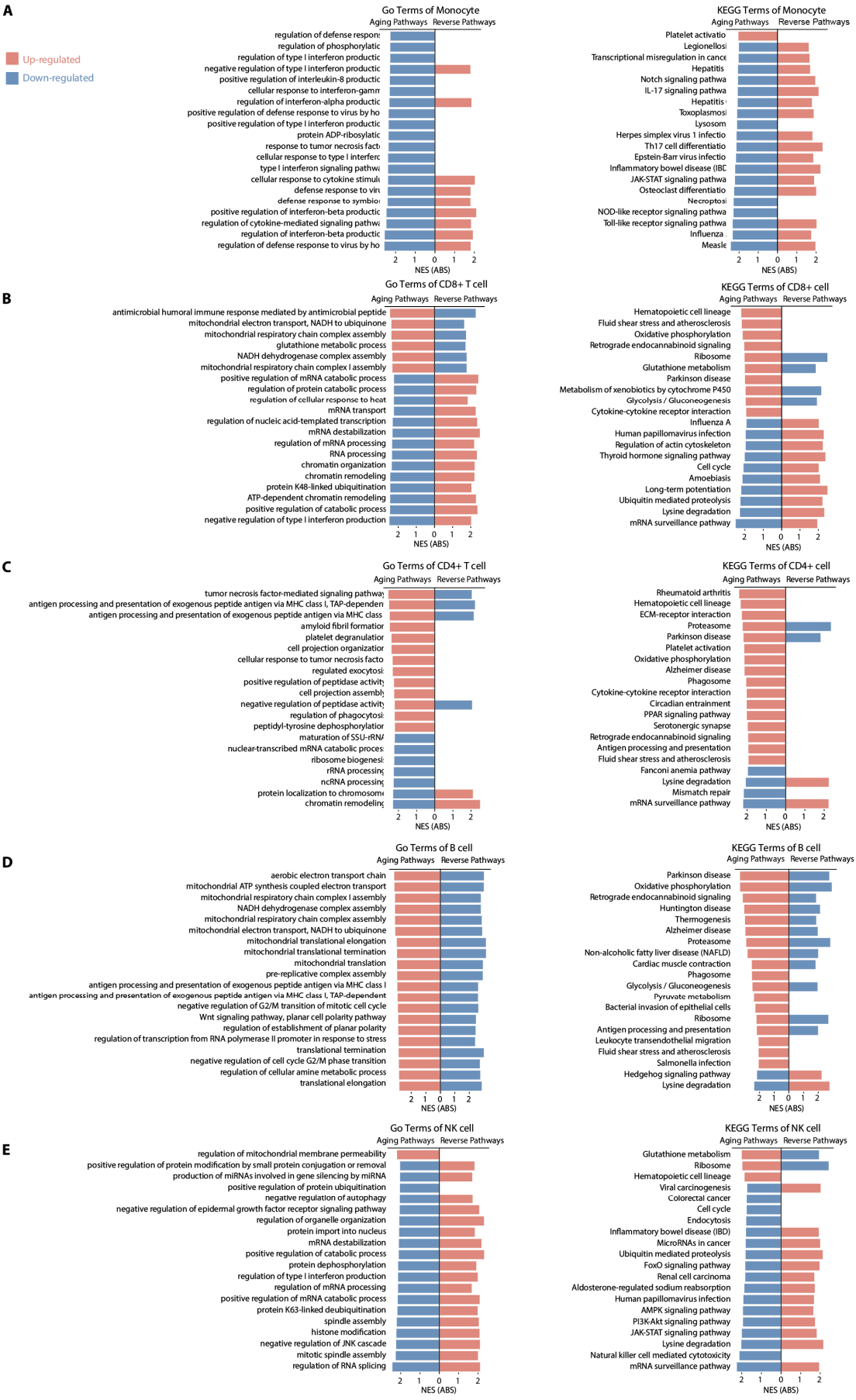
A
Up-regulated
Down-regulated
Go Terms of Monocyte
Aging Pathways
Reverse Pathways
regulation of defense respon
regulation of phosphorylatic
regulation of type I interferon productic
negative regulation of type I interferon productic
positive regulation of interleukin-8 productic
cellular response to interferon-gamm
regulation of interferon-alpha productic
positive regulation of defense response to virus by ho
positive regulation of type I interferon productic
protein ADP-ribosylatic
response to tumor necrosis fact
cellular response to type I interferc
type I interferon signaling pathwa
cellular response to cytokine stimul
defense response to vir
defense response to symbio
positive regulation of interferon-beta productic
regulation of cytokine-mediated signaling pathwa
regulation of interferon-beta productic
regulation of defense response to virus by ho
2 1 0 1 2
NES (ABS)
KEGG Terms of Monocyte
Aging Pathways
Reverse Pathways
Platelet activatio
Legionellosi
Transcriptional misregulation in cance
Hepatitis
Notch signaling pathwa
IL-17 signaling pathwa
Hepatitis
Toxoplasmosi
Lysosom
Herpes simplex virus 1 infectio
Th17 cell differentiatio
Epstein-Barr virus infectio
Inflammatory bowel disease (IBD
JAK-STAT signaling pathwa
Osteoclast differentiatio
Necroptosi
NOD-like receptor signaling pathwa
Toll-like receptor signaling pathwa
Influenza
Measle
2 1 0 1 2
NES (ABS)
B
Go Terms of CD8+ T cell
Aging Pathways
Reverse Pathways
antimicrobial humoral immune response mediated by antimicrobial peptide
mitochondrial electron transport, NADH to ubiquinone
mitochondrial respiratory chain complex assembly
glutathione metabolic process
NADH dehydrogenase complex assembly
mitochondrial respiratory chain complex I assembly
positive regulation of mRNA catabolic process
regulation of protein catabolic process
regulation of cellular response to heat
mRNA transport
regulation of nucleic acid-templated transcription
mRNA destabilization
regulation of mRNA processing
RNA processing
chromatin organization
chromatin remodeling
protein K48-linked ubiquitination
ATP-dependent chromatin remodeling
positive regulation of catabolic process
negative regulation of type I interferon production
2 1 0 1 2
NES (ABS)
KEGG Terms of CD8+ cell
Aging Pathways
Reverse Pathways
Hematopoietic cell lineage
Fluid shear stress and atherosclerosis
Oxidative phosphorylation
Retrograde endocannabinoid signaling
Ribosome
Glutathione metabolism
Parkinson disease
Metabolism of xenobiotics by cytochrome P450
Glycolysis / Gluconeogenesis
Cytokine-cytokine receptor interaction
Influenza A
Human papillomavirus infection
Regulation of actin cytoskeleton
Thyroid hormone signaling pathway
Cell cycle
Amoebiasis
Long-term potentiation
Ubiquitin mediated proteolysis
Lysine degradation
mRNA surveillance pathway
2 1 0 1 2
NES (ABS)
C
Go Terms of CD4+ T cell
Aging Pathways
Reverse Pathways
tumor necrosis factor-mediated signaling pathwa
antigen processing and presentation of exogenous peptide antigen via MHC class I, TAP-dependen
antigen processing and presentation of exogenous peptide antigen via MHC class
amyloid fibril formatior
platelet degranulatior
cell projection organizatior
cellular response to tumor necrosis facto
regulated exocytosi
positive regulation of peptidase activit
cell projection assembl
negative regulation of peptidase activit
regulation of phagocytosi
peptidyl-tyrosine dephosphorylatior
maturation of SSU-rRN
nuclear-transcribed mRNA catabolic proces
ribosome biogenesi
rRNA processin
ncRNA processin
protein localization to chromosom
chromatin remodelin
2 1 0 1 2
NES (ABS)
KEGG Terms of CD4+ cell
Aging Pathways
Reverse Pathways
Rheumatoid arthritis
Hematopoietic cell lineage
ECM-receptor interaction
Proteasome
Parkinson disease
Platelet activation
Oxidative phosphorylation
Alzheimer disease
Phagosome
Cytokine-cytokine receptor interaction
Circadian entrainment
PPAR signaling pathway
Serotonergic synapse
Retrograde endocannabinoid signaling
Antigen processing and presentation
Fluid shear stress and atherosclerosis
Fanconi anemia pathway
Lysine degradation
Mismatch repair
mRNA surveillance pathway
2 1 0 1 2
NES (ABS)
D
Go Terms of B cell
Aging Pathways
Reverse Pathways
aerobic electron transport chain
mitochondrial ATP synthesis coupled electron transport
mitochondrial respiratory chain complex I assembly
NADH dehydrogenase complex assembly
mitochondrial respiratory chain complex assembly
mitochondrial electron transport, NADH to ubiquinone
mitochondrial translational elongation
mitochondrial translational termination
mitochondrial translation
pre-replicative complex assembly
antigen processing and presentation of exogenous peptide antigen via MHC class I
antigen processing and presentation of exogenous peptide antigen via MHC class I, TAP-dependent
negative regulation of G2/M transition of mitotic cell cycle
Wnt signaling pathway, planar cell polarity pathway
regulation of establishment of planar polarity
regulation of transcription from RNA polymerase II promoter in response to stress
translational termination
negative regulation of cell cycle G2/M phase transition
regulation of cellular amine metabolic process
translational elongation
2 1 0 1 2
NES (ABS)
KEGG Terms of B cell
Aging Pathways
Reverse Pathways
Parkinson disease
Oxidative phosphorylation
Retrograde endocannabinoid signaling
Huntington disease
Thermogenesis
Alzheimer disease
Proteasome
Non-alcoholic fatty liver disease (NAFLD)
Cardiac muscle contraction
Phagosome
Glycolysis / Gluconeogenesis
Pyruvate metabolism
Bacterial invasion of epithelial cells
Ribosome
Antigen processing and presentation
Leukocyte transendothelial migration
Fluid shear stress and atherosclerosis
Salmonella infection
Hedgehog signaling pathway
Lysine degradation
2 1 0 1 2
NES (ABS)
E
Go Terms of NK cell
Aging Pathways
Reverse Pathways
regulation of mitochondrial membrane permeability
positive regulation of protein modification by small protein conjugation or removal
production of miRNAs involved in gene silencing by miRNA
positive regulation of protein ubiquitination
negative regulation of autophagy
negative regulation of epidermal growth factor receptor signaling pathway
regulation of organelle organization
protein import into nucleus
mRNA destabilization
positive regulation of catabolic process
protein dephosphorylation
regulation of type I interferon production
regulation of mRNA processing
positive regulation of mRNA catabolic process
protein K63-linked deubiquitination
spindle assembly
histone modification
negative regulation of JNK cascade
mitotic spindle assembly
regulation of RNA splicing
2 1 0 1 2
NES (ABS)
KEGG Terms of NK cell
Aging Pathways
Reverse Pathways
Glutathione metabolism
Ribosome
Hematopoietic cell lineage
Viral carcinogenesis
Colorectal cancer
Cell cycle
Endocytosis
Inflammatory bowel disease (IBD)
MicroRNAs in cancer
Ubiquitin mediated proteolysis
FoxO signaling pathway
Renal cell carcinoma
Aldosterone-regulated sodium reabsorption
Human papillomavirus infection
AMPK signaling pathway
PI3K-Akt signaling pathway
JAK-STAT signaling pathway
Lysine degradation
Natural killer cell mediated cytotoxicity
mRNA surveillance pathway
2 1 0 1 2
NES (ABS)

Fig. S5. Young BMT mitigate aging pathways in senescent immune cells. Go and KEGG functional annotation of the aging and reverse DEGs. In each panel, the left half represents aging DEG-enriched pathways (aging pathway), while the right half represents reverse DEG-enriched pathways (reverse pathway). NES(ABS): absolute normalized enrichment score.

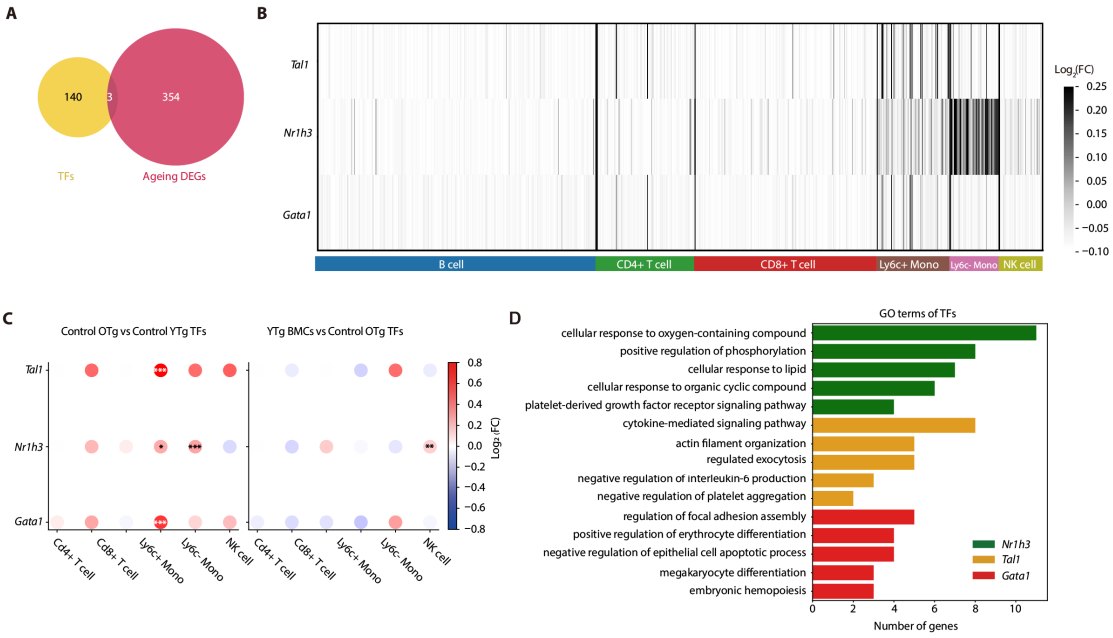

Fig. S6. Transcription factors of the aging and reverse-DEGs analyzed by pseudobulk DEG analysis. (A) Venn plot of the identified transcription factors (TFs) and aging DEGs in PBMCs. (B) Heatmap of the expression level of TFs in each cell type. The color key indicates the Log_2FC values. (C) Dot plots of the effects of aging and young BMT on TF expression. The color key indicates the Log_2FC values. (D) Bar plots of the GO terms enriched by the target genes of Tal1, Nr1h3 and Gata1. The downstream genes of Tal1, Nr1h3 and Gata1 were obtained from the Regulon analysis using SCENIC, and the genes identified through SCENIC analysis may not be DEGs. *indicates $p < 0.05$, **indicates $p < 0.01$, ***indicates $p < 0.001$.

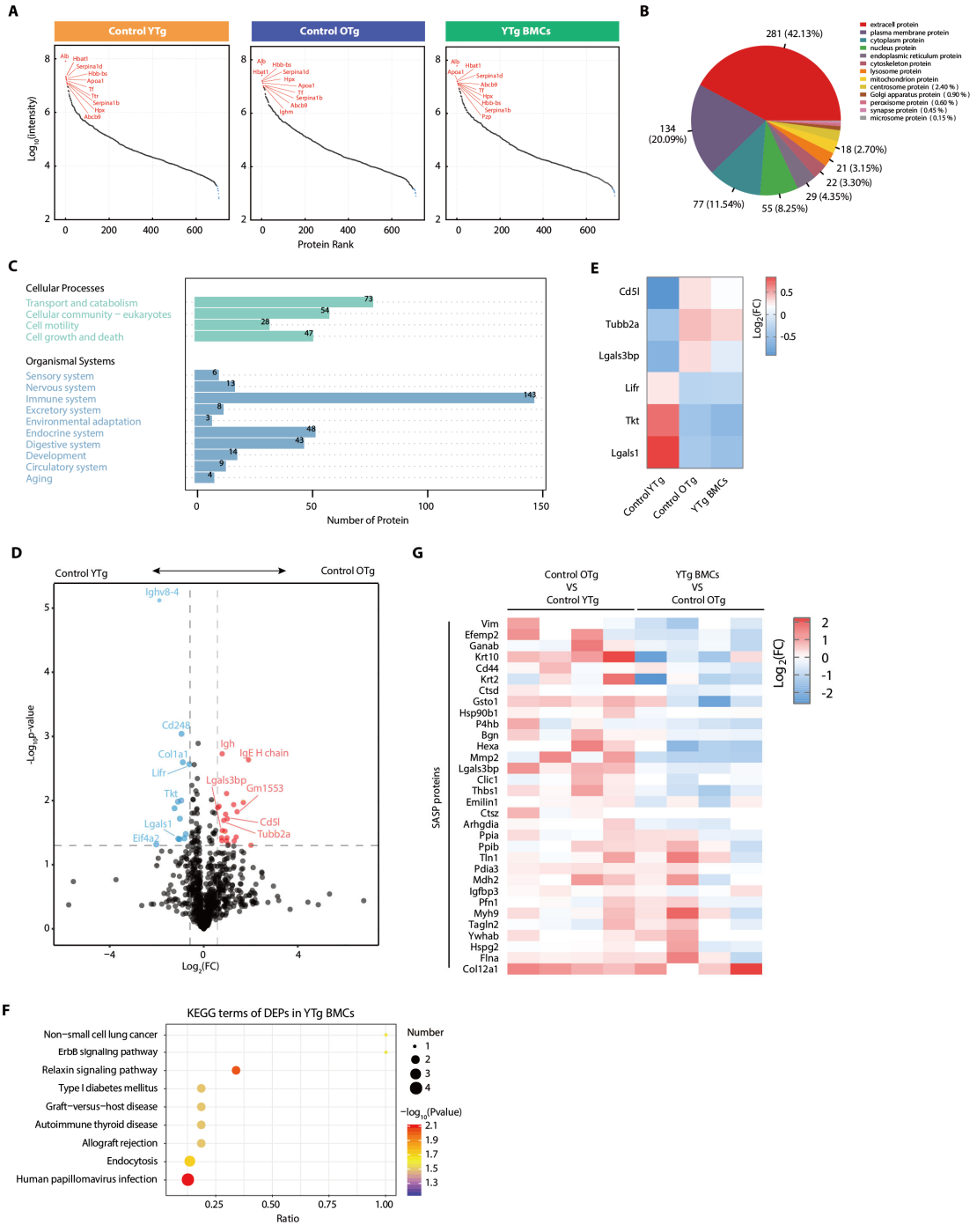

Fig. S7. Young BMT downregulate plasma SASP proteins in aged *APP/PS1* mice. (**A**) Ranked abundances of plasma proteins in the control YTg, control OTg, and YTg BMC groups. (**B**) Subcellular distribution analysis of the plasma proteome. (**C**) KEGG annotation of the cell process and organismal system of the plasma proteins. (**D**)

Volcano map of the protein abundances between control YTg and control OTg. (**E**) Heatmap of the aging-related plasma proteins across the control YTg, control OTg, and YTg BMC groups. The color key indicates the Log_2FC values. (**F**) KEGG functional annotation of differentially expressed proteins (DEPs) in YTg BMC plasma compared to control OTg plasma. Pathways with p-value<0.05 were displayed. (**G**) Heatmap of the SASP proteins across the control YTg, control OTg, and YTg BMC groups. The color key indicates the Log_2FC values.

.

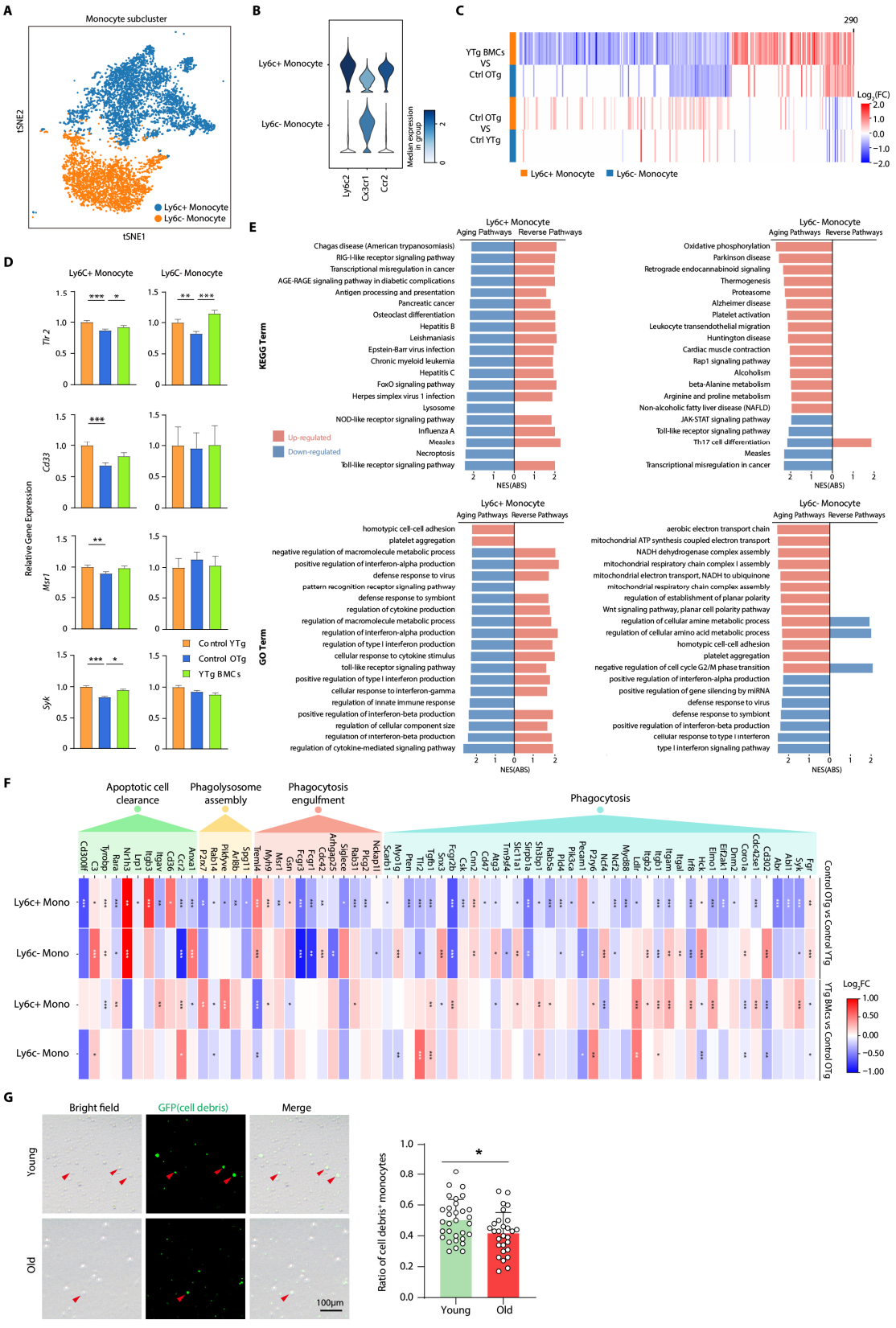

Fig. S8. Analysis of the effects of senescence on different monocyte subtypes. (A)

tSNE projection of monocyte subclusters. (**B**) Violin plot of marker gene expression in monocyte subclusters. (**C**) Heatmap of the aging and reversed DEGs in monocyte subclusters. The color key indicates the log_2FC values. (**D**) Levels of expression of the Aβ uptake-related receptors *Tlr2*, *Cd33*, *Msr1* and *Syk* in monocyte subclusters. One-way ANOVA. (**E**) The GO and KEGG terms enriched by the aging and reverse DEGs in monocyte subclusters. (**F**) Heatmap of phagocytosis related genes in monocyte subclusters. The color key indicates the Log_2FC values. (**G**) Quantification of the levels of cell debris phagocytosis in young and old monocytes. n=30. Un-paired t-test. *indicates $p < 0.05$; **indicates $p < 0.01$, ***indicates $p < 0.001$. The scale bar in g is 100 μm. The error bars are the SEMs.

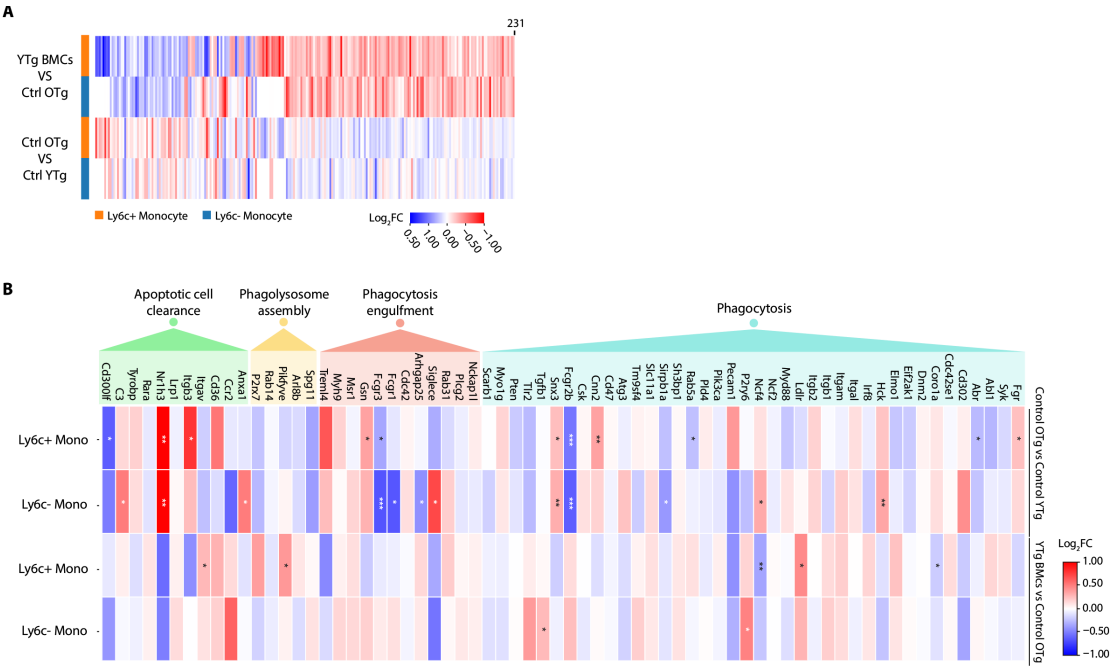

Fig. S9. Aging and reverse-DEGs in different monocyte subclusters analyzed by pseudobulk DEG analysis. (A) Heatmap of the aging and reversed DEGs in monocyte subclusters. The color key indicates the Log_2FC values. (B) Heatmap of phagocytosis related genes in monocyte subclusters. The color key indicates the Log_2FC values. The color indicates the Log_2FC values. *indicates $p < 0.05$, **indicates $p < 0.01$, ***indicates $p < 0.001$.

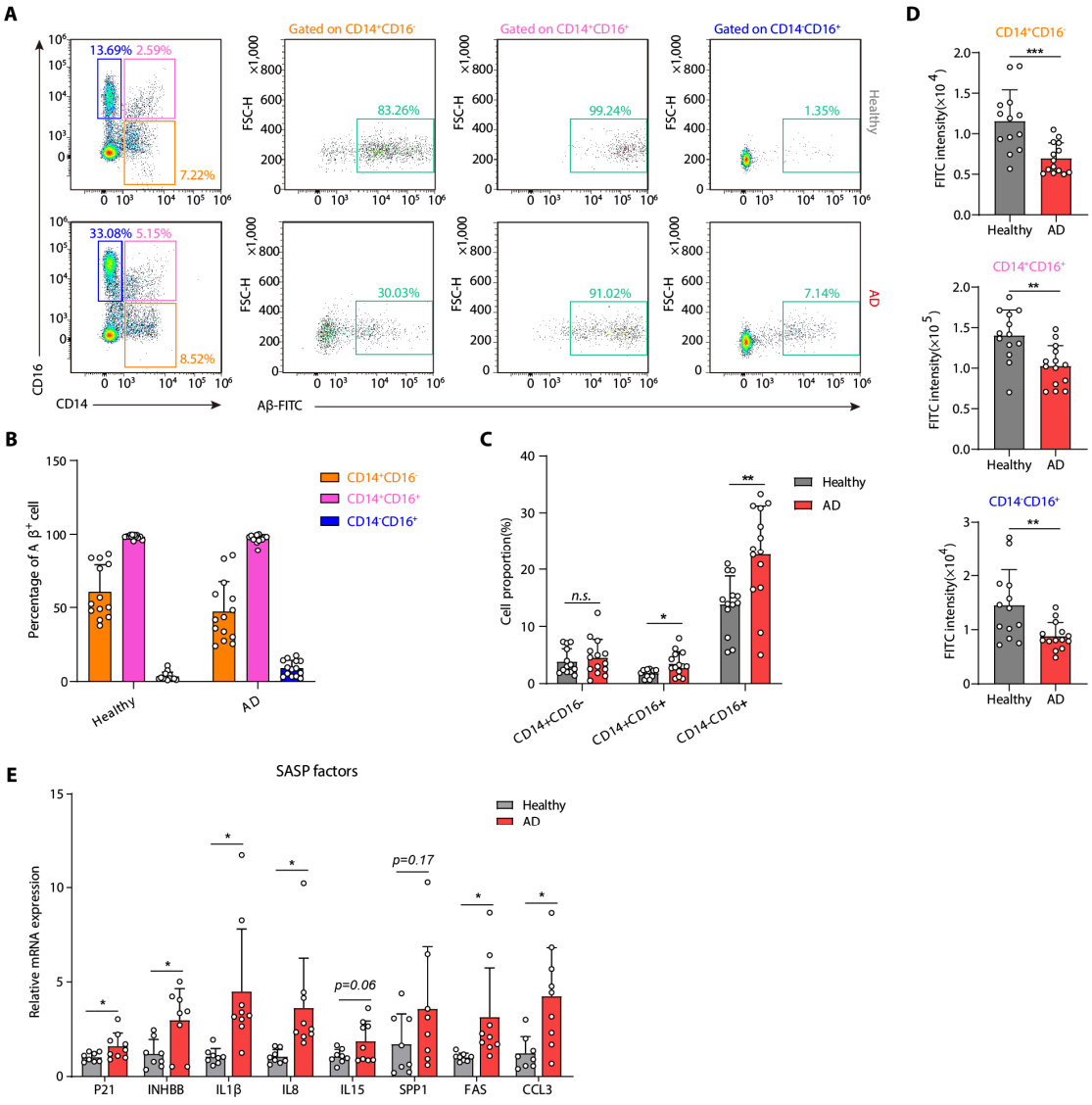

Fig. S10. Comparison of peripheral blood monocytes from AD patients and healthy controls on senescent phenotypes. (**A**) Representative FACS plot of marker gene staining of different monocytes subtypes in AD patients and healthy controls, including classical ($CD14^+CD16^-$), intermediate ($CD14^+CD16^+$), and non-classical ($CD14^-CD16^+$) monocytes. (**B**) Proportion of $A\beta^+$ cells in different monocytes subtypes. (**C**) Proportion of different monocytes subtypes in PBMC from AD patients and healthy controls. Un-paired t-test. (**D**) Quantification of the levels of monocyte Aβ42 uptake in

different monocytes subtypes from AD patients and healthy controls. Un-paired t-test. (**E**) Quantification of senescence marker and SASP factors mRNA level in $CD14^+$ monocytes from AD patients and healthy controls. Un-paired t-test. *indicates $p < 0.05$, ** indicates $p < 0.01$, ***indicates $p < 0.001$. The error bars are the SEMs.

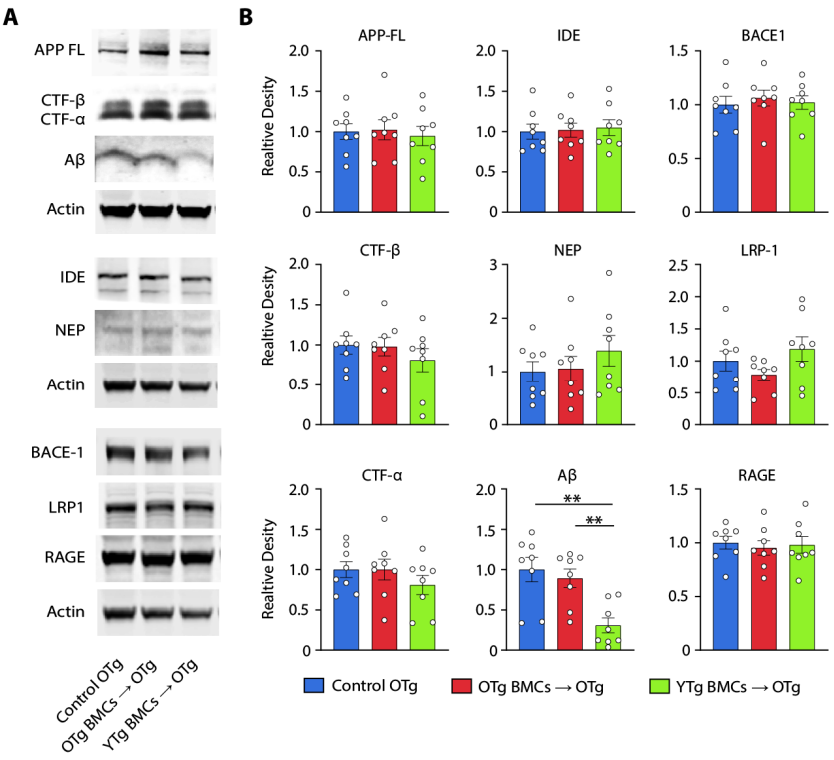

Fig. S11. Quantification of cerebral Aβ metabolism pathway-related proteins. (**A**) Representative western blot image of Aβ metabolism pathway-related proteins in brain homogenates. (**B**) Quantification analysis of Aβ metabolism pathway-related proteins. n=8 per group. One-way ANOVA. **indicates $p < 0.01$, and the error bars are the SEMs.

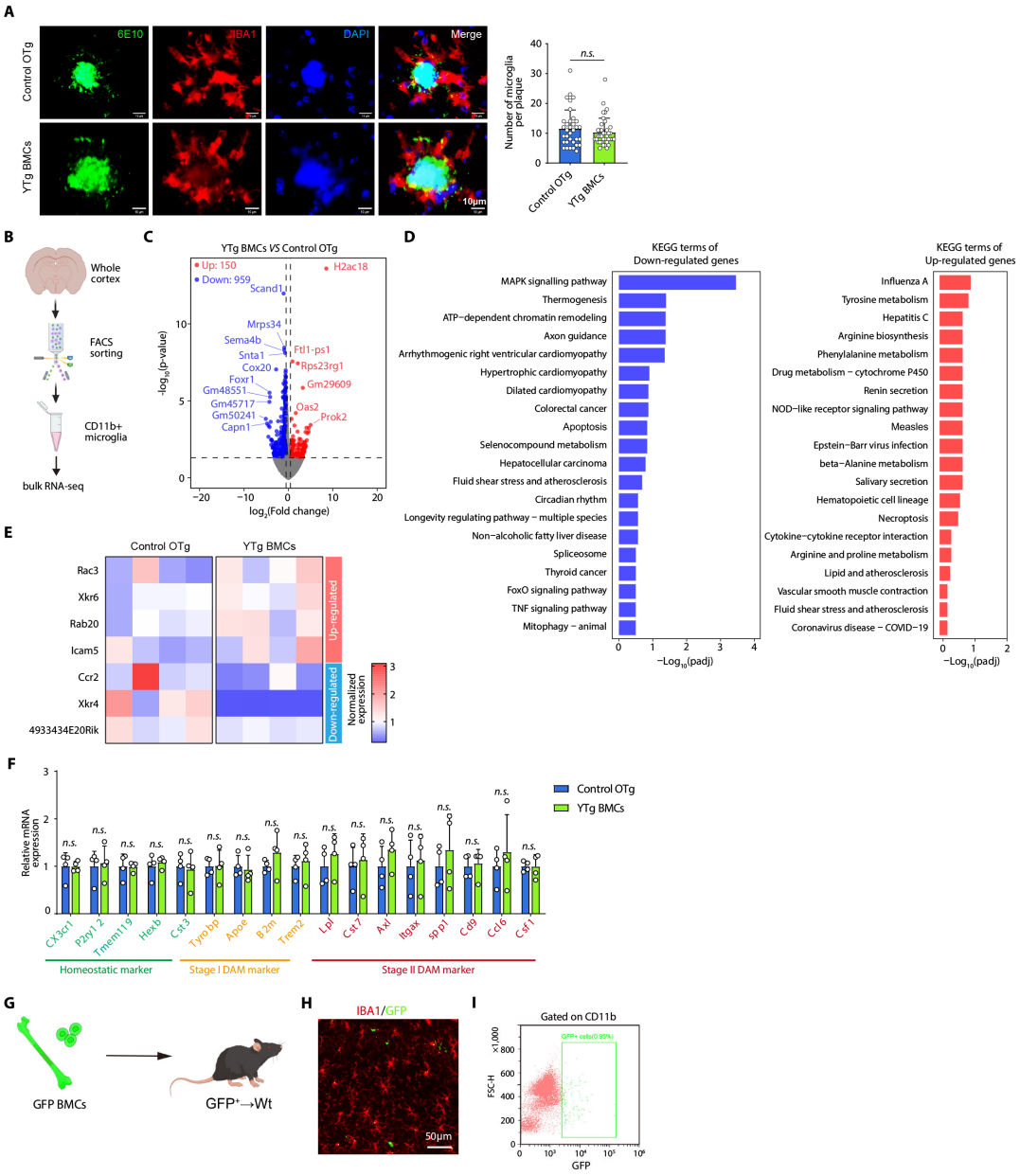

Fig. S12. Effects of young BMT on microglia. (**A**) The number of microglia (Iba-1$^+$, red) within 15 μm of amyloid plaque (6E10, green) in the cortex. Un-paired t-test. (**B**) Schematic of experimental design for RNA-seq analysis. n = 4 per group. (**C**) Volcano plot presenting significantly upregulated (red) and downregulated (blue) (cutoff of $Log_2|FC|>0.5$; p-value < 0.05) genes in YTg BMCs compared to control OTgs. (**D**) Bar plots of the KEGG terms enriched by the DEGs in YTg BMCs microglia compared to

control OTgs. (**E**) Heatmap of significantly differentially expressed genes (p-value < 0.05) involved in phagocytosis related pathways in YTg BMCs and control OTg microglia. Color represents normalized expression value. (**F**) Relative expression of homeostatic and disease associated microglia (DAM) marker genes according to RNA-seq. (**G**) Schematic of experimental design for GFP BMCs transplantation. (**H**) Representative images of cortex in GFP BMCs recipient mice. (**I**) FACS plot of GFP^+ cells gated on $CD11b^+$ channel. The scale bar in a is 10 μm, in h is 50 μm, and the error bars are the SEMs.

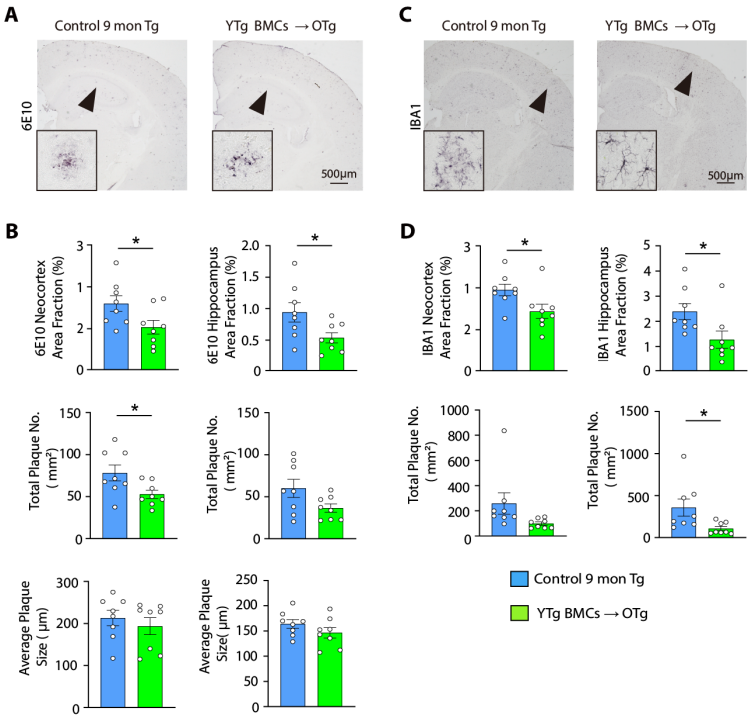

Fig. S13. Comparison of plaque density and microgliosis in YTg BMCs and control 9-month APP/PS1 mice. (**A, B**) Immunostaining and quantification of Aβ plaques stained with 6E10 in the neocortices and hippocampus of YTg BMCs and control 9-month *APP/PS1* mice. Un-paired t-test. (**C, D**) Immunostaining and quantification of microglia stained with IBA1 in the neocortices and hippocampus of YTg BMCs and control 9-month *APP/PS1* mice. Un-paired t-test. n = 8 per group; *indicates $p < 0.05$. The scale bars are 500 μm. The error bars are the SEMs.

Table S3. Characteristics of young and old CN-subjects

	Old (n= 10)	Young (n= 10)	P values
Age, y [mean (SD)]	63.3 (10.9)	27.4 (3.2)	< 0.0001
Male, n (%)	5 (50.0)	7 (70.0)	0.36
Years of education, mean (SD)	10.7 (4.8)	18.5 (2.1)	0.0002
Comorbidities			
Hypertension, n (%)	4 (0.0)	0 (0.0)	0.02
Diabetes mellitus, n (%)	1 (0.0)	0 (0.0)	0.30
Hyperlipidemia, n (%)	2 (0.0)	0 (0.0)	0.14

SD, standard deviation.

Table S4. Demographic data of AD patients and age- and sex-matched CN controls

	AD (n=14)	CN (n=13)	P value
Age, y [mean (SD)]	69.1 (9.7)	67.2 (7.6)	0.55
Male, n (%)	6 (42.8)	6 (46.1)	0.86
Years of education, mean (SD)	10.2 (4.2)	10.8 (3.5)	0.66
MMSE, mean (SD)	13.6 (8.9)	27.1 (2.2)	< 0.0001
CDR, mean (SD)	1.3 (0.9)	0.1 (0.2)	< 0.0001
ADL, mean (SD)	34.3 (13.5)	92 (14.2)	< 0.0001
Comorbidities			
Hypertension, n (%)	3 (21.4)	6 (46.1)	0.17
Diabetes mellitus, n (%)	1 (7.1)	3 (23.1)	0.24
Hyperlipidemia, n (%)	1 (7.1)	1 (7.7)	0.96

AD, Alzheimer's disease; CN, cognitively normal control; SD, standard deviation; MMSE, Mini-Mental State Examination; ADL, Activities of Daily Living; CDR, Clinical Dementia Rating.

174 Table S1. Plasma proteome of all groups

175

176 Table S2. SASP proteins in plasma

17

Table S5. qPCR primers used in this study